

**PAPER****CRIMINALISTICS**

Xiao Hui Tai,<sup>1</sup> M.Stats.; and William F. Eddy,<sup>1</sup> Ph.D.

## A Fully Automatic Method for Comparing Cartridge Case Images\*,†

**ABSTRACT:** When a gun is fired, it leaves marks on cartridge cases that are thought to be unique to the gun. In current practice, firearms examiners inspect cartridge cases for “sufficient agreement,” in which case they conclude that they come from the same gun, testifying in courts as such. A 2016 President’s Council of Advisors on Science and Technology report questioned the scientific validity of such analysis (President’s Committee of Advisors on Science and Technology, Washington, DC, Executive Office of the President). One recommendation was to convert firearms analysis to an objective method. We propose a fully automated, open-source method for comparing breechface marks on cartridge cases using 2D optical images. We improve on existing methodology by automating the selection of marks, and removing the effects of circular symmetry. We propose an empirical computation of a “random match probability” given a known database, which can be used to quantify the weight of evidence. We demonstrate an improvement in accuracy on images from controlled test fires.

**KEYWORDS:** forensic science, firearms identification, cartridge cases, breechface marks, circular symmetry, cross-correlation function

When a gun is fired, it leaves marks on cartridge cases that are thought to be unique to the gun. In current practice, firearms examiners inspect two cartridge cases using a comparison microscope, and if there is “sufficient agreement” between the marks on the cartridge cases, they conclude that they come from the same gun (1), and testify in courts as such. A recent publication by the President’s Council of Advisors on Science and Technology (2) questioned the scientific validity of firearms analysis, making two recommendations for the path forward. The first is to continue improving firearms analysis as a subjective method, by conducting additional black-box studies to determine the reliability of firearms examiners’ conclusions, and also by introducing more rigorous proficiency testing. The second is to convert firearms analysis from a subjective method to an objective method, for example by developing image analysis algorithms to extract signatures and compute degrees of similarity.

Here, we primarily consider the second recommendation, with the current focus being to complement, rather than to replace, subjective methods with objective methods. There has been research by various groups with regard to objective methods. In recent years, the National Institute of Standards and Technology (NIST) has been advocating the use of 3D topographies for

measurement (3), coupled with algorithms that are largely automated (4,5). 3D topography measurements are in contrast to 2D optical (grayscale) images, the latter being older technology that has been used in investigations since as early as 1932 (6). More recently, law enforcement agencies have been using 2D imaging as part of the National Integrated Ballistics Information Network (NIBIN), a program started by the Bureau of Alcohol, Tobacco, Firearms and Explosives (ATF) in 1999. NIBIN is a national database of ballistic evidence, including cartridge cases recovered at crime scenes, as well as from test fires from firearms recovered in shooting investigations and from individuals. Firearms examiners enter images into NIBIN using a platform developed by Forensic Technology WAI, Inc. (FTI), of Montreal, Canada, which captures a 2D optical image of the “questioned” casing. The system then performs a search of the database and returns a list of top ranked potential matches using a proprietary algorithm. The examiner uses this list to determine on which physical cartridge cases to focus their efforts. They retrieve those that they view are the best potential matches, and examine them using a comparison microscope to evaluate if they are indeed matches.

The main reason for NIST’s recommendation to use 3D topographies is that optical images are sensitive to lighting conditions, whereas 3D topographies are a direct measurement of surface contours. As part of a report by NIST in 2007 assessing the feasibility of developing a national ballistics imaging database (7), an algorithm for comparing 3D topographies of cartridge cases was developed. The accuracy of this method was compared to FTI’s proprietary algorithm, concluding that 3D topographies could potentially produce much more accurate results. Following NIST’s lead, other groups have also developed algorithms for comparing 3D topographies [see e.g., (8)].

Despite these developments, there remains interest in 2D optical images among both practitioners and researchers. One reviewer commented that for practitioners, many crime

<sup>1</sup>Department of Statistics, Carnegie Mellon University, Baker Hall 132, Pittsburgh, PA 15213.

\*Presented at the Forensics @ NIST 2016 Conference, November 8–9, 2016, in Gaithersburg, MD; and at the 48th Annual Training Seminar of the Association of Firearm and Tool Mark Examiners (AFTE), May 14–19, 2017, in Denver, CO.

†Partially funded by the Center for Statistics and Applications in Forensic Evidence (CSAFE) through Cooperative Agreement #70NANB15H176 between NIST and Iowa State University, which includes activities carried out at Carnegie Mellon University, University of California Irvine, and University of Virginia.

Received 24 Mar. 2017; and in revised form 17 May 2017; accepted 18 May 2017.

laboratories have continued to use 2D imaging due to the high cost of equipment for acquiring 3D topographies, as well as the lack of field-wide accepted and validated methods which are necessary to maintain accreditation. For researchers, both the continued and historical use of 2D imaging mean that the majority of data in local and national databases are in 2D, and it is essential for algorithms to be effective on these. Recent work on algorithms for 2D images includes a paper by NIST applying their Congruent Matching Cells method, originally developed for 3D topographies, to 2D (9), as well as work by Roth et al. (10) on images involving operational datasets taken from a police department, in addition to a data set of controlled test fires, as is usually used by researchers.

Here, we extend the literature on 2D comparisons by improving on existing algorithms, introducing a method that is both fully automated and open source; the code is available as an R software package at <https://github.com/xhtai/cartridges>. The original comparison of performance of 2D with 3D (7) was made using proprietary algorithms on the 2D images, and we revisit one of the datasets used, to determine if the performance using 2D images remains as poor. To our knowledge, this dataset has not been studied since the 2007 paper.

There has also been ongoing research as to how to compute likelihood ratios from cartridge case comparisons, so that they may be incorporated with other evidence [see e.g., (8,11)]. Here, we propose a method to compute “random match probabilities” empirically, given a known database. This method was developed for 2D comparisons but is also applicable to 3D.

## Materials and Methods

### Data

The cartridge cases used are the same ones collected and analyzed in NIST’s 2007 study, and a detailed account of the experiment can be found in (7). The cartridge cases were re-imaged by NIST at their Gaithersburg, Maryland campus, and the data were made available as part of the Ballistics Toolmark Research Database (<https://tsapps.nist.gov/NRBTD>), an open-access research database of fired bullet and cartridge reference data. Briefly, there were a total of 108 cartridge cases, collected from test fires of 4 Ruger P95D, 4 S&W 9VE, and 4 Sig Sauer P226 pistols. Each was fired 9 times using 3 each of 3 different brands of ammunition: PMC, Remington, and Winchester. These were imaged using a Leica FS M reflectance microscope with ring light illumination. The objective was 2×, and the resolution was 2.53 μm, and images are 1944 × 2592 pixel grayscale files in PNG format. As in (7), we refer to these images as the NBIDE (NIST Ballistics Imaging Database Evaluation) dataset.

To analyze these data, we will treat each image in turn as the “new” or “questioned” image, and the remaining 107 images as the known database. We perform 107 pairwise comparisons for each new image, for a total of 107\*108 or 11,556 pairwise comparisons. For each pairwise comparison, we will compute a similarity score and the probability of obtaining a higher score by chance.

### Steps for One Pairwise Comparison

The following are proposed steps for making one pairwise comparison. Steps 1 through 4 are preprocessing steps, 5 computes a similarity score and 6 a “random match probability.”

- Automatically select breechface marks by removing the non-primer areas and the firing pin impression.
- Level image to adjust for nonuniform lighting caused by the surface being tilted on a plane
- Remove circular symmetry to adjust for nonuniform lighting caused by the surface having differences in depth that are circular in nature.
- Outlier removal and filtering to highlight certain features.
- Maximize correlation by translations and rotations.
- Compute the probability of obtaining a higher score by chance given a known database.

These steps build on methodology published in (7) and implemented in (10). There are three main improvements: steps 1, 3, and 6 above. Each step is explained in detail in the following subsections.

### *Automatically Select Breechface Marks*

The first step is to automatically select the breechface marks. In NIBIN (7) and other research (9,10), this step is performed manually by adjusting a larger circle to pick out the primer region, and a smaller circle for the firing pin impression. Here, we select the breechface marks automatically by first finding the primer region and then removing the firing pin impression. We do not constrain either region to be circular, and this is especially important for the firing pin impression, which could have different shapes depending on the make and model of the gun. A rough schema for finding the primer region is given in Fig. 1.

To remove the firing pin impression, we use a similar set of steps, but we start with an edge detector to first identify the firing pin region. We use a Canny edge detector (12) because it allows the specification of two thresholds, which enables weaker edges to be detected, if they are connected to a strong edge. This is very useful in detecting the firing pin impression, because not the entire border may be prominently marked. The steps are shown in Fig. 2.

Next, we perform a second pass where we apply an edge detector again with slightly different parameters, to try to remove any remaining marks. This is necessary for some images where parts of the firing pin impression might not be as highly contrasted with the surrounding breechface impression, resulting in them being missed the first time. This different set of parameters picks up such edges that are connected to the previously identified firing pin impression. The steps are in Fig. 3.

### *Level Image to Adjust for Nonuniform Lighting*

The second step is to level the image. As explained in (7) and (10) this step is necessary because the base of the cartridge case may not be level, and may instead be tilted slightly on a plane. As a result, images of such a surface may have differences in brightness that are planar in nature. We fit a plane that captures these differences, and then take the residuals, which ensure that the resulting image is free from planar differences in brightness. An example is in Fig. 4.

### *Remove Circular Symmetry to Adjust for Nonuniform Lighting*

The next step is to remove the effects of circular symmetry. Analogous to step 2, the base of the cartridge case could have differences in depth that are circular in nature, for example the surface may slope inwards toward the center. This would cause

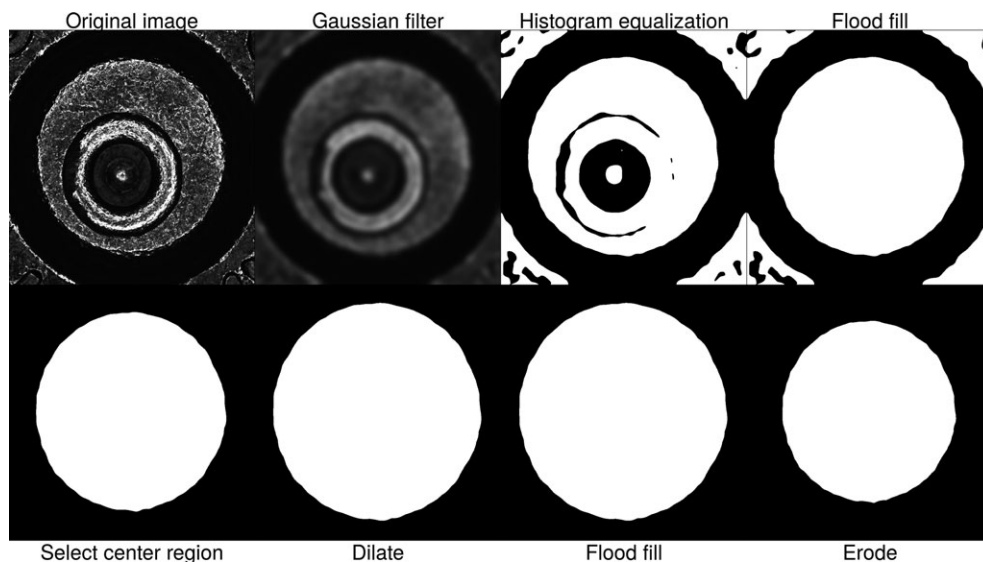


FIG. 1—Series of steps to find the primer region for an example image. This image is from a Ruger gun, firing a PMC cartridge. In some images, the firing pin impression is so close to the edge of the primer that the center region selected is not circular, and the last three steps (dilating, filling, and eroding) ensure that we get a region that is close to circular.

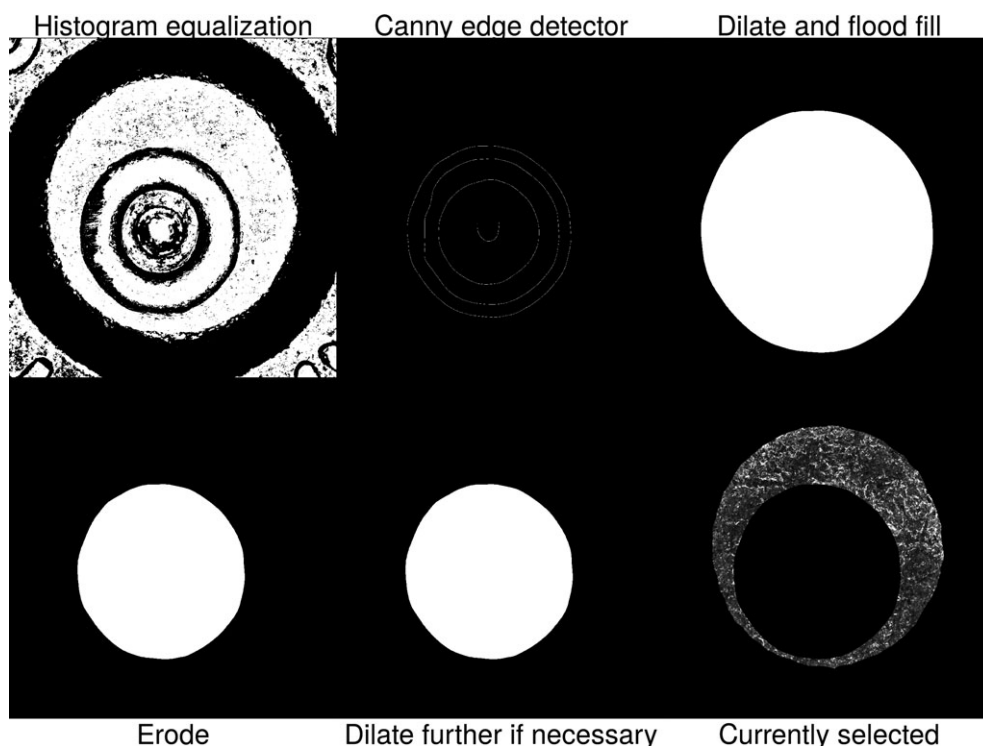


FIG. 2—Series of steps to find the firing pin impression of the example image.

corresponding differences in brightness such as the center of the image being darker than the edges. As in the previous step, we fit a model that captures this circular symmetry, and then take the residuals. The residuals will be free from any circular symmetry.

The model that we fit is a linear combination of circularly symmetric basis functions (13). Briefly, this model assumes that pixels located the same distance from the center of the image take the same value, and each basis function corresponds to a unique distance from the center. The coefficient for each basis

function is the mean of pixel values for pixels with the corresponding distance from the center. We ignore missing pixels and only use values that are available. Because of the large number of basis functions, with each only containing only a few pixels, the variance of the coefficients is large, and we fit a local smoother through the coefficients to get a smoothed circularly symmetric model. The results are in Fig. 5.

The fitted model and the residuals are in Fig. 6. These residuals are free from both planar bias from the previous step, and circular symmetry.

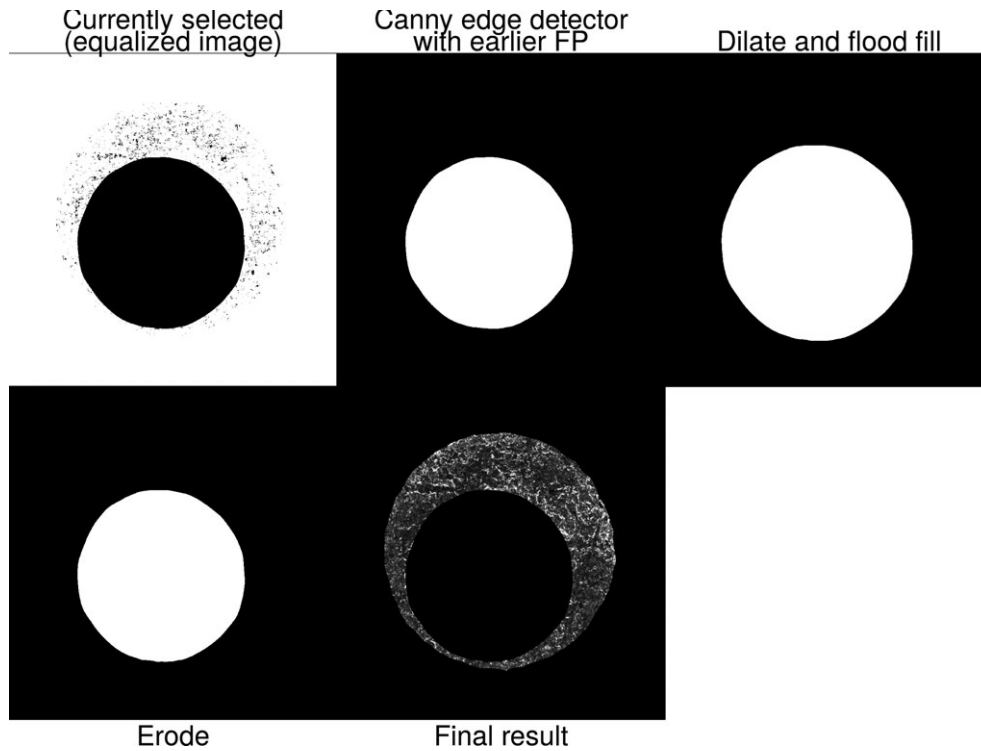


FIG. 3—Here, we run the edge detector a second time. In this particular example, the entire firing pin impression has already been removed, so these steps do not produce any effect, and the image remains unchanged.

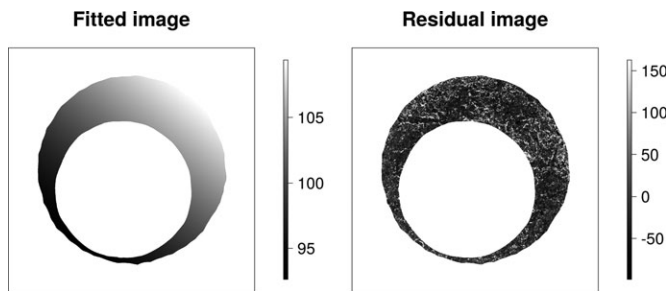


FIG. 4—We have the fitted plane on the left and the residuals on the right. In this example, the original image is slightly darker in the bottom left corner and brighter on the top right. The residuals are free from any such effects. We take the residuals for further processing.

#### Outlier Removal and Filtering

The last preprocessing step is outlier removal and filtering. Again this follows the methodology of (7) and (10). Outliers are removed and filled in (14) so as not to affect the similarity scores being computed, and filtering highlights certain features of the image. The resulting image after all preprocessing is on the left in Fig. 7.

#### Maximize Correlation by Translations and Rotations

After preprocessing, step 5 computes a similarity metric. Here, we use the maximum cross-correlation function ( $CCF_{\max}$ ), used in (4) and (10). For each rotation angle, we compute

$$CCF(I_1, I_2) = \frac{\sum_{i,j} I_1(i,j) I_2(i+dy, j+dx)}{\sqrt{\sum_{i,j} I_1(i,j)^2} \sqrt{\sum_{i,j} I_2(i,j)^2}},$$

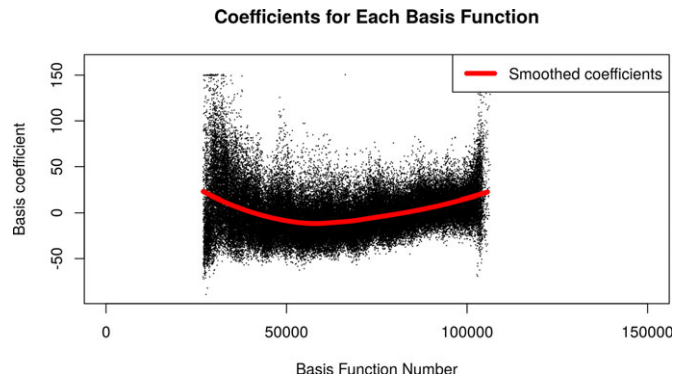


FIG. 5—Fitted coefficients for our example image. [Color figure can be viewed at [wileyonlinelibrary.com](http://wileyonlinelibrary.com)]

where  $I_1$  and  $I_2$  are the two images,  $i$  indexes the rows and  $j$  indexes the columns, and  $dx$  and  $dy$  represent translations. The CCF is a matrix of correlation values, where each entry corresponds to a particular translation, and we store the maximum correlation. We repeat for rotation angles 2.5 degrees apart, and then .5 degrees apart in the neighborhood of the highest correlation. The maximum correlation between two images is known as the  $CCF_{\max}$ . An example is in Fig. 7.

#### Compute Probability of Obtaining a Higher Score by Chance Given a Known Database

In the final step, we convert each similarity score into a statement of probability, specifically a “random match probability” given a known database. Both (11) and (8) propose methods for computing likelihood ratios, which are a ratio of the densities of



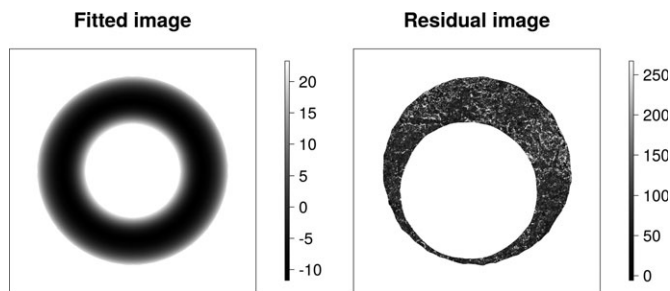


FIG. 6—Fitted circularly symmetric model and resulting residuals.

similarity scores using nonmatch versus match distributions. In (11), a parametric distribution applicable to all guns is proposed, while (8) proposes case-specific distributions, determined empirically by conducting test fires for each make and model of gun.

Here, we focus on the denominator of the likelihood ratio, and propose a method to compute the probability of obtaining a higher score by chance, empirically, given a known database. This method can be applied to all guns. These probabilities attach meaning to the scores, and also serve as a measure of uncertainty for this comparison procedure.

In theory, we assume that all  $CCF_{\max}$  values for nonmatches are drawn from the same distribution, and given such a distribution, we compare each newly computed score against this distribution, and compute the right tail proportion. This value is the probability of observing a higher  $CCF_{\max}$  by chance. In reality, the assumption might not hold, and we would not have access to the theoretical distribution of all  $CCF_{\max}$  values. We might instead have a known database, where we are able to compute all pairwise nonmatching scores. These form a sample from the unknown distribution, and an illustration is in Fig. 8. For example, using the NBIDE dataset, for each new image we have a database of 107 images, and doing all pairwise comparisons within this database, we have a total of 10,494 nonmatch scores, which would form a sample from the unknown population of nonmatch scores. We can then compare a calculated similarity score against this distribution.

## Results

### All Pairwise Comparisons

As described in the Data section, we do all pairwise comparisons for each of the 108 images in the dataset, for a total of 11,556 comparisons. As we know the true identity of all the

$CCF_{\max}$  for nonmatches

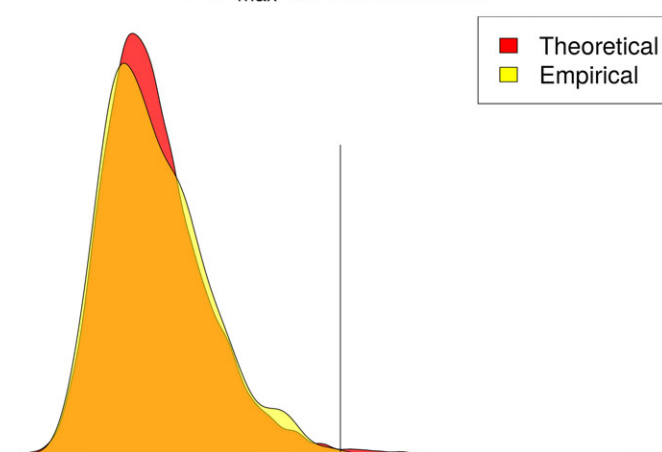


FIG. 8—The darker distribution is the theoretical distribution of  $CCF_{\max}$  values for nonmatches, which we do not know. The other distribution shown is the empirical distribution constructed from the values computed using a known database. The vertical line represents a new  $CCF_{\max}$  value. To compute the probability of observing a higher score than this, we take the proportion of the empirical distribution to the right of the vertical line. [Color figure can be viewed at [wileyonlinelibrary.com](http://wileyonlinelibrary.com)]

images, we are able to group the comparisons into true matches and nonmatches. The distributions of  $CCF_{\max}$  values split by true matches and nonmatches are in Fig. 9. The two distributions overlap, meaning that this method is unable to perfectly separate the true matches from the nonmatches using a single cutoff for  $CCF_{\max}$ .

We also look at the probabilities obtained in step 6, and again we group the results by true matches and true nonmatches. The results are in Fig. 10. For the true matches, ideally the probabilities should be small, indicating that the  $CCF_{\max}$  values are large enough that the probability of getting a larger score by chance is small. Here for about 80% of the observations, the probabilities are actually zero, because some of the similarity scores for the true matches are much larger than the largest observed value for true nonmatches, as seen in Fig. 9. There are several probabilities close to 1, which correspond to the points in the left part of the overlapping regions in Fig. 9.

### Comparison with Other Results

As described earlier, we have added two preprocessing steps: the automatic selection of breechface marks and the removal of

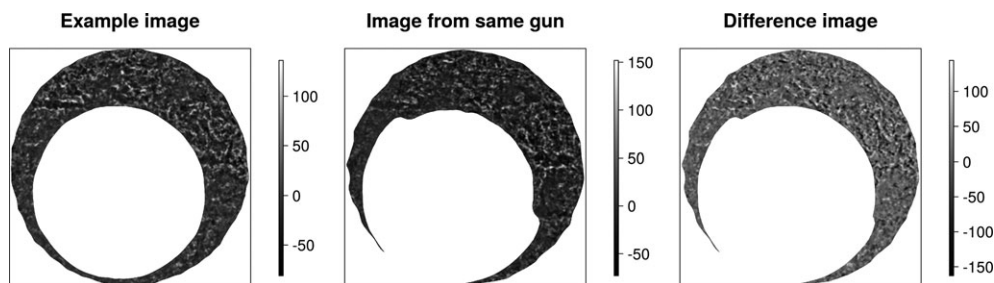


FIG. 7—We compare our example image (on the left) against another image from the NBIDE study, which was obtained using the same gun. We obtain a similarity score of .36, with a rotation angle of  $-15$  degrees, meaning that the second image is rotated 15 degrees counterclockwise. Plotting the two images with the second rotated, we notice that the breechface marks are now lined up well. We also compute the difference between the two images, and this is plotted on the far right.

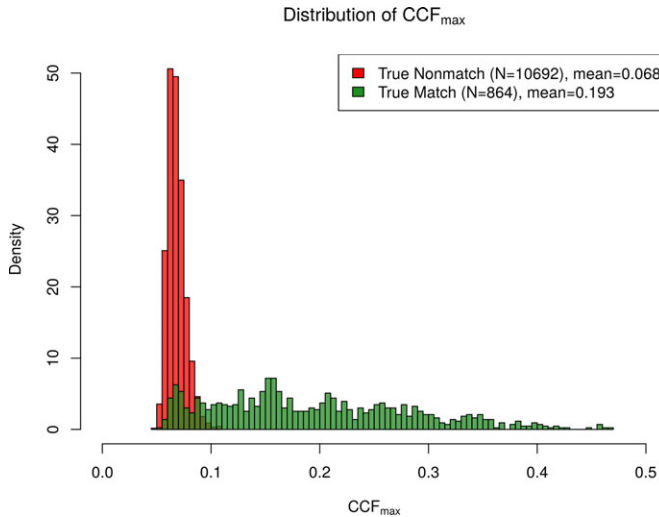


FIG. 9—The true nonmatch  $CCF_{max}$  distribution has a much smaller mean and variance than the distribution for true matches, but there is not a clear separation between the two. This means that some true matches do not produce very high similarity scores. [Color figure can be viewed at [wileyonlinelibrary.com](http://wileyonlinelibrary.com)]

circular symmetry. We compare the similarity scores with those without the addition of these steps, and the results are in Fig. 11. From the plot in the center, it is fairly obvious that removing circular symmetry has on average little impact on the similarity scores for true matches. For the true nonmatches, there are more points below the 45-degree line (in fact, over 2/3 of the points), indicating that removing circular symmetry reduces scores for nonmatches. This is illustrated more clearly in Fig. 12. For the true matches, the individual marks are similar enough that even after any circular symmetry is removed, the images remain highly correlated.

To determine the effect of automatically selecting the breech-face marks, we consider the first plot in Fig. 11. There is a linear relationship between the two sets of results, but one noticeable difference is that each score on the horizontal axis

corresponds to a range of observed scores on the vertical axis, and the positive correlation is not as strong. The scores in general are higher because they are above the 45-degree line. This is especially true for the true matches, and if we were to draw a best fit line for only the true matches, we notice that this is above the 45-degree line. The effect on the true nonmatches is less obvious, and an argument can be made for there being little to no effect.

Putting the two together, we get the last plot in Fig. 11. We see a weaker linear relationship, higher scores for the true matches, and slightly lower scores for the true nonmatches, although the effect is not as pronounced as in the second plot.

As a final step, we compare the results to those in (7). The metric that Vorburger et al. used to evaluate performance on the 2D algorithm was the number of matches in the “top 10 list.” For each new image, there are 107 images in the known database, and the top 10 list is the list of 10 images that have the highest similarity scores when compared against the new image. The maximum possible number of true matches in the top 10 list is 8, and this represents the best result. We produce this same metric using the similarity scores we calculate after pre-processing using different methods, and the results are in Table 1.

The performance of published methods is markedly better than NIBIN, but we note that the latter were obtained in 2007 and might not be an accurate reflection of current NIBIN technology. Although we see that our proposed methodology is an improvement over other 2D methods, we do not achieve the accuracy of 3D topographies for this dataset.

## Discussion

### Computing Random Match Probabilities

In computing the probabilities of observing a higher  $CCF_{max}$  value by chance in step 6, we apply the same calculation to all makes and models of guns. We might believe that depending on the two images being compared, the nonmatch distributions might differ; for example if the two images come from the same

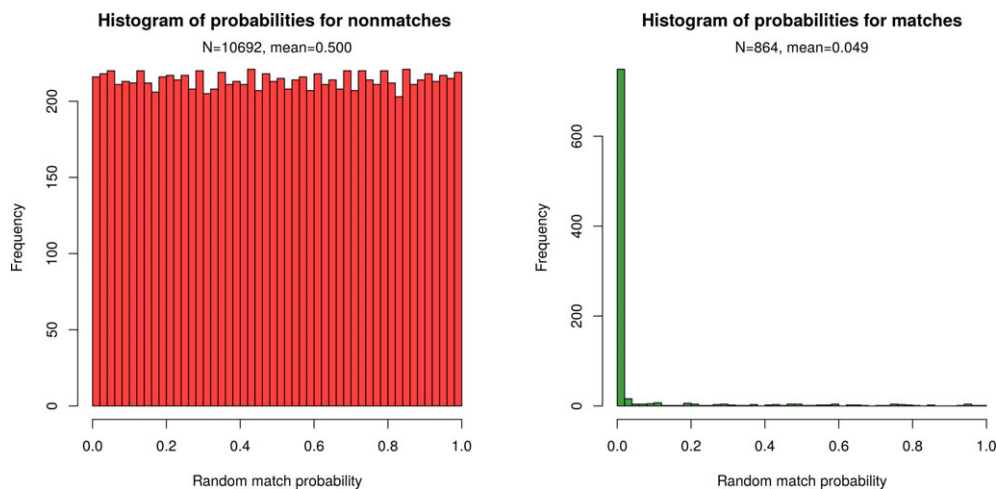


FIG. 10—The true nonmatch probabilities follow a roughly uniform distribution, which is to be expected. (We can think of the random match probabilities in the context of the hypothesis test, with the null being that the images do not come from the same gun, and the alternative being that they do. The calculated probabilities are p-values in the context of this hypothesis test. The  $CCF_{max}$  values of true nonmatches should then come from the null distribution, and statistical theory tells us that the p-values follow a uniform distribution.) The true matches have low probabilities of obtaining a higher score by chance, which is a good result. [Color figure can be viewed at [wileyonlinelibrary.com](http://wileyonlinelibrary.com)]

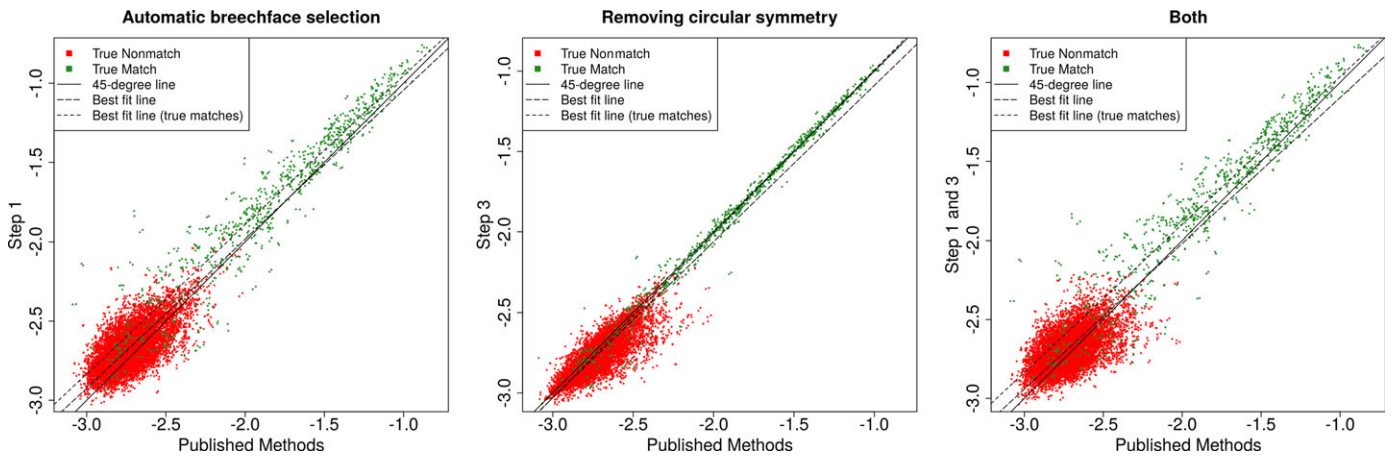


FIG. 11— $CCF_{max}$  values for all pairwise comparisons using different sets of preprocessing steps are plotted. Published methods on the horizontal axis refer to the preprocessing steps being a manual selection of breechface marks, leveling, outlier removal, and filtering. The logarithmic scale is used on both axes to highlight the differences in the lower values. [Color figure can be viewed at [wileyonlinelibrary.com](http://wileyonlinelibrary.com)]

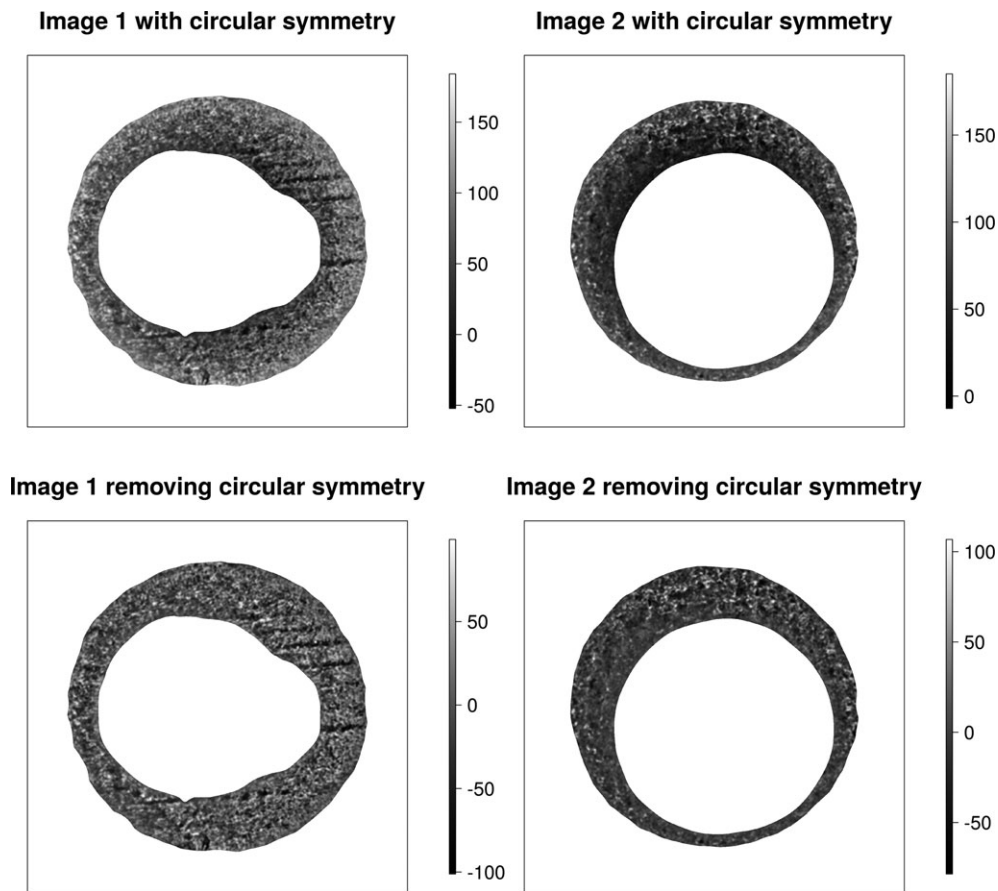


FIG. 12—This example illustrates the effect of removing circular symmetry. We compare the images on the left respectively with those on the right. In the images on the first row, we added the same circular symmetry to both images, causing them to be darker in the center and getting brighter toward the edges. The similarity score in this case is .72. On the second row, this circular symmetry is removed and the score drops to just .04, because the individual marks are not very similar.

make and model of gun and cartridge, the  $CCF_{max}$  values might be higher. The correct interpretation of the probability that was computed in step 6 is an average over all possible identities of the two images involved. Here, we examine the nonmatch distributions in greater detail, and suggest possible refinements of this probability calculation.

We consider the nonmatch distribution in Fig. 9. This can be broken up in different ways: by individual gun, by gun brand, by gun, and cartridge brand, as well as by type of comparison, and we would like to see if there are differences in the distributions. As an example, the distributions by type of comparison are in Fig. 13. If we were to do formal statistical tests, such as

TABLE 1—Comparison of the number of true matches in “top 10 lists” for various methodologies. All rows except the last use 2D optical images.

Methodology	8	7	6	5	4	3	2	1	0
NIBIN in 2007 (7)	13	25	23	19	13	9	5	1	0
Published methodology (7,10)	58	19	14	10	2	2	1	2	0
Proposed methodology	68	21	7	1	4	3	2	2	0
Only add step 1	67	19	7	4	4	3	2	1	1
Only add step 3	60	21	12	6	4	2	2	1	0
3D (7)	101	7	0	0	0	0	0	0	0

the Kolmogorov–Smirnov test, we do see significant differences in distributions. Although some of these differences might be statistically significant but not practically significant, it is possible that nonmatch distributions depend on both the image in the database, as well as the new image.

To make a more accurate probability statement, instead of averaging over all possible comparisons, it might be better to compare against an empirical distribution that is of the same type as the new comparison being made. However, in an actual comparison against a known database, the identity of the new image is unknown, so we are unable to determine which nonmatch distribution the computed  $CCF_{\max}$  value is

coming from. We propose two alternatives. The first is to construct different empirical nonmatch distributions, for each gun–cartridge combination found in the known database. For example, if we have Ruger-PMC images in the database, we construct a nonmatch distribution for Ruger-PMC based on all nonmatch comparisons in the database involving Ruger-PMC. When comparing a new image to any Ruger-PMC image in the database, we produce a similarity score, and compare this to the Ruger-PMC nonmatch distribution that we just constructed. This would give us the probability of obtaining a higher score by chance, given that one image in the comparison is a Ruger-PMC. This probability might be interpreted as an average over all possible identities of the new image (instead of over both images).

Alternatively, based on Fig. 13, we might expect that the nonmatch similarity scores are the highest for comparisons where both the gun and cartridge brand are the same. A conservative approach would be to only use these comparisons to form the empirical nonmatch distribution. Every new comparison would be compared to this distribution, and the probabilities might then be interpreted as an upper bound: The probability of obtaining a larger similarity score by chance is less than  $p$ , where  $p$  is the probability computed in this fashion.

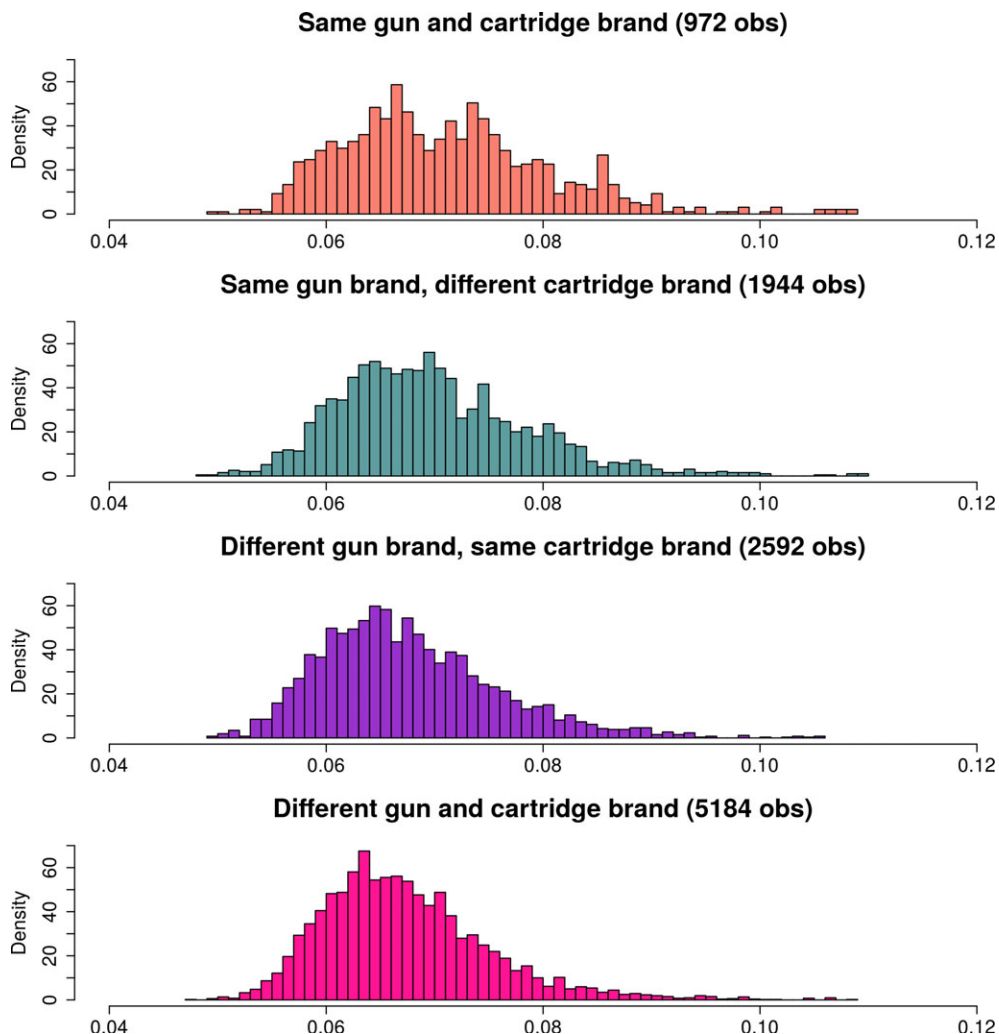


FIG. 13—Breaking up the distribution of  $CCF_{\max}$  values for nonmatches by type of comparison. The distribution for comparisons involving the same gun and cartridge brand is shifted slightly to the right. [Color figure can be viewed at [wileyonlinelibrary.com](http://wileyonlinelibrary.com)]



## Conclusion

We have proposed an improvement of existing methodology for comparing 2D optical images of breechface impressions. This algorithm is fully automated and open source, and provides improved accuracy. Accuracy, however, does not reach the level of 3D topographies for this dataset. This could be because the marks left on the cartridge cases were insufficiently pronounced to be adequately captured using 2D ring light photography, whereas these marks were captured in 3D topographies. Another point to note is that the methodology that we improved upon is not the only existing methodology, but it is arguably the most established. Our proposed changes are to the preprocessing steps and can be applied to different similarity metrics or registration procedures [e.g., (5,10)]. Similarly, our proposed empirical method of computing “random match probabilities” given a known database can be adapted to different similarity metrics and also to 3D topographies.

There remain aspects of this work that would benefit greatly from further investigation. For one, it should be tested much more extensively using images from different guns and cartridges. Parameters used in the various steps should be adjusted carefully. The code should be optimized for speed, and methods for dealing with large databases should also be looked into. Results should be compared to that made by human examiners.

Eventually, in practice, such an algorithm could be used by firearms examiners as a tool for blind verification, as well as for reporting uncertainty. Given a “questioned” cartridge case, examiners might first use currently established methods for determining matches. Then, they could run the proposed algorithm using an image of the questioned cartridge case and some given database. An ideal result would be if the matching cartridge case(s) picked out by the examiner also has (have) the highest similarity score(s) returned by the algorithm. When reporting the evidence in court, the examiner could then report her conclusion of a match, together with the probability of observing a higher similarity score by chance, given the database that she is working with, as estimated using the algorithm. Alternatively, an examiner may also wish to attach an objective measure to a single comparison, without considering a database search. This might be for a particular pair of cartridge cases that she has found to be a matched pair. For such purposes, a single pairwise comparison of the associated images using the proposed algorithm could be used.

## Acknowledgments

We would like to thank Xiaoyu Alan Zheng at NIST for collecting the data and for advice. We also thank many others at NIST for their advice and comments, especially Robert M. Thompson for reviewing our manuscript. We thank Joseph Roth

and his co-authors at Michigan State University for sharing the code they used in (1), and finally the anonymous reviewers for their helpful comments.

## References

1. AFTE Criteria for Identification Committee. Theory of identification, range of striae comparison reports, and modified glossary definitions—an AFTE criteria for Identification Committee report. *AFTE J* 1992;24(2):336–40.
2. President’s Committee of Advisors on Science and Technology. Report to the President on forensic science in criminal courts: ensuring scientific validity of feature-comparison methods. Washington, DC: Executive Office of the President, 2016.
3. Song J, Chu W, Vorburger TV, Thompson R, Renegar TB, Zheng A, et al. Development of ballistics identification – from image comparison to topography measurement in surface metrology. *Meas Sci Technol* 2012;23(5):054010.
4. Weller TJ, Zheng A, Thompson R, Tulleners F. Confocal microscopy analysis of breech face marks on fired cartridge cases from 10 consecutively manufactured pistol slides. *J Forensic Sci* 2012;57(4):912–7.
5. Song J. Proposed, “NIST Ballistics Identification System (NBIS)” based on 3D topography measurements on correlation cells. *AFTE J* 2013;45(2):184–94.
6. Heard BJ. Firearms - bullet and cartridge case identification: a brief history of firearms identification. Chichester, U.K.: John Wiley & Sons Ltd, 2009.
7. Vorburger T, Yen J, Bachrach B, Renegar T, Filliben J, Ma L, et al. Surface topography analysis for a feasibility assessment of a national ballistics imaging database. Gaithersburg, MD: National Institute of Standards and Technology, 2007;NISTIR 7362.
8. Riva F, Champod C. Automatic comparison and evaluation of impressions left by a firearm on fired cartridge cases. *J Forensic Sci* 2014;59(3):637–47.
9. Tong M, Song J, Chu W, Thompson RM. Fired cartridge case identification using optical images and the congruent matching cells (CMC) method. *J Res Nat Inst Stand Technol* 2014;119:575–82.
10. Roth J, Carrievau A, Liu X, Jain AK. Learning-based ballistic breech face impression image matching. In: *Proceedings of the 2015 IEEE 7th International Conference on Biometrics Theory, Applications and Systems (BTAS); 2015 Sept 8-11; Arlington, VA. Piscataway, NJ: IEEE: 2015;1–8; <http://ieeexplore.ieee.org/stamp/stamp.jsp?tp=&number=7358774&isnumber=7358743> (accessed April 28, 2017).*
11. Song J. Proposed, “congruent matching cells (CMC)” method for ballistic identification and error rate estimation. *AFTE J* 2015;47(3):177–85.
12. Canny J. A computational approach to edge detection. *IEEE Trans Pattern Anal Mach Intell* 1986;6:679–98.
13. Zeifman LE. A new parametric model for the point spread function (PSF) and its application to hubble space telescope data [dissertation]. Pittsburgh, PA: Carnegie Mellon University, 2014.
14. D’Errico J. Inpaint\_nans. 2004, MATLAB central file exchange; [https://www.mathworks.com/matlabcentral/fileexchange/4551\\_inpaint\\_nans](https://www.mathworks.com/matlabcentral/fileexchange/4551_inpaint_nans) (accessed April 28, 2017).

Additional information and reprint requests:

Xiao Hui Tai, M.Stats.  
Department of Statistics  
Carnegie Mellon University  
Baker Hall 132  
Pittsburgh  
PA 15213  
E-mail: xtai@andrew.cmu.edu